Current Eye Research

ISSN: (Print) (Online) Journal homepage: https://www.tandfonline.com/loi/icey20

Biomechanical Effects of Two forms of PGF2α on ex-vivo Rabbit Cornea

Rong Zhu , XiaoBo Zheng , LiLi Guo , YiPing Zhao , Yuan Wang , Jie Wu , AYong Yu , JunJie Wang , FangJun Bao & Ahmed Elsheikh

To cite this article: Rong Zhu , XiaoBo Zheng , LiLi Guo , YiPing Zhao , Yuan Wang , Jie Wu , AYong Yu , JunJie Wang , FangJun Bao & Ahmed Elsheikh (2020): Biomechanical Effects of Two forms of PGF2α on ex-vivo Rabbit Cornea, Current Eye Research, DOI: 10.1080/02713683.2020.1805771

To link to this article: https://doi.org/10.1080/02713683.2020.1805771

Accepted author version posted online: 14 Aug 2020.

Publisher: Taylor & Francis

Journal: *Current Eye Research*

DOI: 10.1080/02713683.2020.1805771

Biomechanical Effects of Two forms of PGF2α on ex-vivo Rabbit Cornea

Authors

Rong Zhu [1], XiaoBo Zheng [1,2], LiLi Guo [1], YiPing Zhao [3], Yuan Wang [1], Jie Wu [1], AYong Yu [1], JunJie Wang [1,2 *], FangJun Bao [1,2*], Ahmed Elsheikh [4,5,6]

Rong Zhu and XiaoBo Zheng are co-first authors of the article.

Affiliations

[1] Eye Hospital, Wenzhou Medical University, Wenzhou 325027, China

[2] The Institution of Ocular Biomechanics, Wenzhou Medical University, Wenzhou 325027, China

[3] Department of Ophthalmology, Ninth People's Hospital, Shanghai JiaoTong University School of Medicine, No.639 ZhizaojuRoad, Shanghai, 200025, China

[4] School of Engineering, University of Liverpool, Liverpool L69 3GH, UK

[5] National Institute for Health Research (NIHR) Biomedical Research Centre for Ophthalmology, Moorfields Eye Hospital NHS Foundation Trust and UCL Institute of Ophthalmology, London, UK

[6] Beijing Advanced Innovation Center for Biomedical Engineering, Beihang University, Beijing, China

Conflict of Interest

The authors declare no conflict of interest. The funders had no role in the design of the study; in the collection, analyses, or interpretation of data; in the writing of the manuscript, or in the

decision to publish the results.

Running title

Biomechanical influence of PGF2α on rabbit cornea

Financial Support

This study was supported by the Zhejiang Provincial Natural Science Foundation of China under Grant (LY20H120001, LQ20A020008), the National Natural Science Foundation of China (31771020), the Projects of Medical and Health Technology Development Program in Zhejiang Province (2019RC056, 2018KY541, 2016ZHB012), the Science and Technology Plan Project of Wenzhou Science and Technology Bureau (Y20180172, Y20170198, Y20170792) and the General Projects of Department of Education of Zhejiang Province (Y201839651).

Contributors

All authors have read and agree to the published version of the manuscript. Conceptualization, J.W. (Junjie Wang) and F.B.; methodology, R.Z., and A.Y.; software, X.Z. and A.E.; validation, R.Z. and Y.Z.; formal analysis, R.Z. and F.B.; investigation, Y.W.; data curation, X.Z., L.G. and J.W. (Jie Wu); writing – original draft, R.Z. and F.B.; writing – review & editing, J.W. (JunJie Wang), F.B. and A.E.; supervision, J.W. (JunJie Wang), F.B. and A.E.; funding acquisition, X.Z., J.W. (JunJie Wang) and F.B.

Co-Corresponding author

Dr. JunJie Wang

No. 270 Xueyuan West Road, WenZhou City, ZheJiang Prov, 325027, China

e-mail: w.wangjunjie@outlook.com

Tel: 86-577-88067937; Fax: 86-577-88824115

Corresponding author

Dr. FangJun Bao

No. 270 XueYuan West Road, WenZhou City, ZheJiang Prov, 325027,China
e-mail: bfjmd@126.com
Tel: 86-571-88193999; Fax: 86-571- 86795926

PRECIS:

PGF2α can decrease the collagen fibril density and cause remodeling of the extracellular matrix in ex-vivo rabbit cornea, both of which lead to a stiffness reduction in corneal tissue.

Abstract

Purpose: To investigate the biomechanical effects of two synthetic prostaglandin F2α analogues (PGF2α), namely Travoprost and Tafluprost, on the ex-vivo rabbit cornea.

Materials and Methods: 96 eyes of 48 Japanese white rabbits were divided into 3 equal groups randomly; the Travoprost treated group (Tra), the Tafluprost treated group (Taf) and the control group (Co). Eyes in Tra and Taf groups were preserved in storage medium for 10 days with 1:10 Travoprost and Tafluprost diluents, respectively; while the Co eyes were preserved in a similar but PGF2α-free medium. 24 corneas of each group were tested under inflation conditions with up to 30 mmHg posterior pressure. The pressure-deformation data obtained experimentally were used in an inverse analysis process to derive the stress-strain behavior of the tissue, using which the tangent modulus, a direct measure of the tissue's material stiffness, was calculated. The remaining 8 specimens of each group were analyzed using electron microscopy for fibril diameter and interfibrillar spacing.

Results: Although the central corneal thickness increased significantly in the three groups after storage ($p< 0.01$), it was similar in all groups both before ($p= 0.598$) and after storage ($p= 0.181$). After treatment with Travoprost and Tafluprost, the corneas exhibited lower tangent modulus (by 29.2% and 29.8%, respectively at 6 kPa stress) and larger stromal interfibril spacing (by 21.9% and 23.6%) compared with the control group. There was no significant change in fibril diameter with either Travoprost or Tafluprost treatment ($p= 0.769$).

Conclusions: The results demonstrated significant reductions in tangent modulus and increases in interfibrillar spacing, which were of similar magnitudes, with the application of two different forms of PGF2α.

Keywords: prostaglandin; cornea; biomechanics; stromal fibril; inverse analysis

Introduction

Glaucoma is one of the leading causes of irreversible blindness, associated with destructions in ganglion cells and fibers, and leading to a gradual loss in visual field [1, 2]. The risk of glaucoma progression could be reduced through reductions in intraocular pressure (IOP) [3], using either pharmacologic therapy or surgical solutions. Prostaglandin F2α analogues (PGF2α) are among the most commonly prescribed classes of topical hypotensive agents, and are frequently used as first-line monotherapy for patients with open angle glaucoma or ocular hypertension [4]. As glaucoma is a chronic condition that requires long-term therapy, the effect of these drugs on corneal performance, including its biomechanical behavior, needs to be well understood.

Corneal stiffness, depicting the corneal resistance to deformation under internal or external forces, principally depends on the ocular geometry and thickness as well as the micro-architecture of the tissue and the biomechanics of its constituent components. The main load-carrying components of corneal tissue are the collagen fibrils, which form an important part of the stroma's extracellular matrix and control the shape of the cornea under loads such as the IOP. PGF2α upregulate the activity of matrix metalloproteinase (MMP) and downregulate the inhibitors of MMP (TIMP) [5-7] – both effects decrease the collagen fibril density (or increase fibril spacing) and remodel the extracellular matrix in the cornea, ciliary body and sclera [8, 9]. While these changes can cause a reduction in IOP through enhancing the aqueous humor outflow – through the uveoscleral pathway to the suprachoroidal space and to episcleral veins [10, 11]– they can also affect corneal biomechanics and hence the measurement of IOP.

Previous studies have reported that topical therapy with PGF2α (Travoprost 0.004% and Tafluprost 0.0015%) induce significant reductions in CCT, which may be a result of remodeled extracellular matrix [12-14]. This effect would be expected to induce reductions in corneal mechanical stiffness, possibly introducing underestimations in IOP measurements and inaccuracies in procedures (such as refractive surgeries) that interact mechanically with corneal tissue [15]. This study seeks to quantify the changes in corneal biomechanics caused

by the usage of two forms of PGF2α, namely Travoprost and Tafluprost, through experimental testing and microstructural characterization of ex-vivo rabbit corneas that have been treated with these agents.

Materials and methods

2.1 Experimental animals

48 Japanese white rabbits (2-3 kg) were included in this study, all from the Animal Breeding Unit of Wenzhou Medical University (WMU). The animals were treated in line with the ARVO Statement for Use of Animals in Ophthalmic and Vision Research, and every effort was made to minimize suffering. The study was approved by the Animal Care and Ethics Committee of the Eye Hospital of WMU.

2.2 Experimental design

The rabbits were euthanized by intravenously injecting high concentrations of pentobarbital sodium (Merok, Germany), following which the bilateral eyes (total 96 eyes) were enucleated. The corneal and a 3-mm ring of scleral tissues were extracted with all other ocular components removed. The specimens were randomly divided into three groups (namely the Tra group, Taf group and control group, Co) of 32 eyes each. A process was followed to ensure that no bilateral eyes from the same rabbit were included in the same group. Tra and Taf groups were placed for 10 days in storage medium Eusol-C (Alchimia S.r.l, Ponte S. Nicolo`, Italy) with Travoprost (Travatan, 0.004%, Alcon Laboratories, Inc., Fort Worth, TX) or Tafluprost (Tapros, 0.0015%, Santen Pharmaceutical Co,Ltd, Japan) diluent (1:10 dilution of stock solution). The 32 specimens of the Co group were placed in the same medium but without any PGF2α. The 1/10 dilution was selected to enable comparison with earlier studies [16, 17] and to reflect the discrepancy between the comparatively short storage duration adopted herein and the long-term usage in clinical practice. All specimens were incubated under conditions of 37°C and 5% CO_2 for 10 days as in a previous study [18]. Corneal thickness at 16 regularly distributed points, along four main meridians (horizontal, vertical, 45^o and 135^o) was measured before storage, at end of storage period and just before testing using an ultrasonic pachymeter (SP-3000, Tomey Inc, Nagoya, Japan). Corneal diameter was

measured using a Vernier caliper in the same four directions.

2.3 Biomechanical Inflation Testing

Briefly, 24 corneas of each group were mounted onto a custom-built pressure chamber where mechanical clamps were used to ensure tight edge connection along the ring of scleral tissue of the specimen. The pressure chamber was filled with PBS and connected to a syringe pump to control the pressure inside the chamber. A differential pressure transducer (DMP-HS, Hangzhou, China) was adopted to monitor the real-time pressure in the chamber. A laser beam (LK series, Keyence, Milton Keynes, UK) was used to capture the displacement of corneal apex with 0.05 micron resolution. The experimental procedure illustrated in Figure 1 has been described in a previous study [19]. Side images (Figure 1A) of each cornea were captured at different loading levels (0, 4, 8 mmHg, etc) by three cameras (EOS 60D, Canon, Inc. Tokyo, Japan) arranged around the specimen with angles 75°, 195° and 316° measured from the right horizontal direction (Figure 1B). The anterior profiles were identified from the camera images using Image J software (version 1.45s, National Institutes of Health, USA) with 10 micron resolution. This process was used to determine the initial shape of specimen used later in construction of numerical models.

To stabilize the behavior, the specimens were conditioned through three cycles of loading and unloading up to a pressure of 30 mmHg, applied at a rate of 0.10 mmHg/s. These values were selected as they were slightly higher than the IOP level and the IOP change rate commonly seen in rabbit eyes as indicated in our previous studies [19, 20]. A recovery time of 90 seconds was allowed between successive loading cycles to ensure the behavior was free of effect of the strain history of repeated loading cycles [21],[22]. Within this period, the specimens were able to recover at least 95% of their apical deformation under the maximum applied posterior pressure. Finally, the specimens underwent a fourth loading cycle up to 30 mmHg, the results of which were used in subsequent inverse analysis to determine the material properties of the tissue.

2.4 Inverse Analysis

An inverse analysis process was used to obtain the mechanical properties of corneal tissue based on the experimental pressure-deformation results as described in previous studies [19, 22]. Seventy-two, specimen-specific finite element (FE) models, each employing 1728, fifteen-node triangular prism elements (C3D15H), arranged in twelve rings and two layers, were developed for the inverse analysis from the initial geometries of the specimens, given by their thickness, cross-sectional images and limbal diameter measurements [19] (Figure 1C). An encastre boundary condition was applied along the limbus in the FE models to mimic the connection to the mechanical clamps in the experimental test.

Each cornea model was assumed to have the same material behavior across its surface and across the thickness. This assumption was adopted to simplify comparisons between different specimen groups. For the same reason, a first-order hyperelastic Ogden constitutive model [19, 20, 23] was used to represent corneal material behavior with a strain energy function expressed as:

$$W = \frac{2\mu}{a^2}\left(\overline{\lambda_1}^{\alpha} + \overline{\lambda_2}^{\alpha} + \overline{\lambda_3}^{\alpha} - 3\right) + \frac{1}{D}(J-1)^2 \quad (1)$$

where W represents the strain energy per unit volume, $\overline{\lambda_k}$ the deviatoric principal stretches = $J^{-1/3} \times \lambda_k$ (k=1, 2, 3), λ_1, λ_2, λ_3 the principal stretches, $J = \lambda_1\lambda_2\lambda_3$. Material parameters μ and α are the strain hardening exponent and the shear modulus, respectively. D is the compressibility parameter expressed by $= \frac{3(1-2\nu)}{\mu(1+\nu)}$ and calculated with the corneal tissue assumed to be nearly incompressible [24],[25] and a Poisson's ratio, ν, of 0.48 [19].

The inverse analysis process employed Abaqus, a finite element software package (Dassault Systèmes Simulia Corp., Rhode Island, USA) and optimization software LS-OPT (Livermore Software Technology Corp, CA, USA) as described in previous studies [19, 20]. Essentially, the analysis determined the optimal values of the material parameters μ and α for each cornea by minimizing the root mean square (*RMS*) error between the experimental and numerical displacements at the corneal apex using the following objective function:

$$RMS = \sqrt{\frac{1}{P}.\sum_{p=1}^{P}(\delta_p^{exp} - \delta_p^{num})^2}$$

where P is the total number of pressure levels at which the *RMS* is calculated (i.e. 2, 4, … up to 30 mmHg), and δ_p^{exp} and δ_p^{num} represent the experimental and numerical displacements of the corneal apex at pressure level p.

Within the inverse analysis, parameters μ and α could take values ranging from 0.001 to 0.1, and from 50 to 250, respectively. The parameter ranges were suitable for analysis of all specimens in this study. Solution uniqueness was evaluated using 3 specimens (one randomly selected from each group), by repeating the inverse analysis four more times while starting with initial values that were double and half the values used in the first attempt.

2.5 Histological Analysis

To determine the effect of treatment with PGF2α on collagen fibril diameter and interfibrillar spacing, 8 corneas from each group were fixed with 2.5% glutaraldehyde, embedded in Epon (SPI-PON 812 Kit, SPI-CHEM, PA, USA), sectioned on the sagittal plane and stained with uranyl acetate and lead citrate. Five 50nm-thick sections were extracted from each cornea and were analyzed by a professional pathologist (Shen LJ) using a transmission electron microscope (TEM, H-7500, Hitachi, Japan) with ×40,000 magnification. The information of fibrils was measured in the middle surface of the stroma (300μm away from epithelium). The TEM images were assessed using image processing software, Image J (National Institute of Health, USA) to determine the mean diameter of fibrils and the mean interfibrillar spacing as described in a previous study [20]. Only fibrils showing circular or elliptical borders with high contrast were included in the fibril diameter calculations [26]. On the other hand, the calculation of interfibrillar spacing (W) was based on:

$$\mathrm{W} = \sqrt{\mathrm{Area/number\ of\ fibrils}} - \mathrm{mean\ fibril\ diameter}.$$

The mean values of interfibrillar spacing and fibril diameter obtained from the five TEM images obtained for each specimen were used in subsequent analyses.

2.6 Statistical analysis

All statistical analysis was performed using the PASW Statistics 20.0 (SPSS Inc., Chicago, USA). One-way analysis of variance (ANOVA) or Kruskal-Wallis H test was carried out to compare the biomechanical and geometrical parameters among the three groups according to a normal distribution test. p values less than 0.05 were considered indicative of statistical significance.

Results

3.1 Corneal thickness

The central corneal thickness of Tra, Taf and Co groups was 342.2±24.2 μm, 349.5±19.0 μm and 343.4±32.6 μm, respectively, pre-storage, and 698.4±130.6 μm, 686.8±90.3 μm and 748.1±133.0 μm post storage. No significant differences were found in corneal thickness among the three groups before storage ($p= 0.598$) or after storage ($p= 0.181$), even though the thickness increases with storage were significant in all three groups ($p< 0.01$). The peripheral corneal thickness after storage and corneal diameter were 708.9±118.1 μm and 11.2±0.2 mm for the Tra group, 667.5±112.4 μm and 11.0±0.4 mm for the Taf group, and 722.4±99.8 μm and 11.1±0.2 mm for the Co groups. The difference among the three groups was not statistically significant ($p> 0.05$).

3.2 Pressure deformation behavior

Figure 2 shows the pressure-apical displacement behavior of the corneas under cycle loading. A notable stiffness increase in all specimens was observed from the first to second loading cycle as indicated by a displacement reduction of 13.5±3.7% on average over the loading range. A similar comparison between the 2nd and 3rd cycles, and between 3rd and 4th cycles showed displacement reduction ratios of 3.7±2.1% and 1.4±1.5%, respectively. These results justified the use of 4th cycle results as representative of the specimens' repeatable behavior. The max apical displacements in the 4th cycle ranged between 0.38 and 0.99 mm (0.55±0.14 mm) in the Tra group, 0.24 and 0.84 mm (0.50±0.12 mm) in the Taf group, and 0.17 and 0.58 mm (0.37±0.11 mm) in the Co group. The mean pressure-apical displacement behavior of the

three specimen groups are plotted in Figure 3. All specimens exhibited nonlinear pressure-displacement behavior at low pressure levels before it changed to almost linear at a pressure between 7 and 15 mmHg.

3.3 Inverse analysis results

Inverse analysis was employed to derive a constitutive model for each cornea that matched the best (lowest RMS) with the experimental results in terms of pressure-displacement behavior. The study started with an exercise to assess the uniqueness of the material parameters obtained from the inverse analysis procedure in 3 specimens (1 from each of the three groups). The process started with an analysis that used the initial values: $\mu = 0.001$ and $\alpha = 90$, then repeated the analysis with each of these initial values doubled and/or halved, Table 1. The final parameter values obtained from the three analyses are listed in Table 1. The results demonstrated that the inverse analysis procedure adopted in the study was robust in arriving at unique material parameters in each case. Following this, the material parameters μ and α for each specimen in each specimen group were obtained and their mean values are given in Table 2.

With the material parameters determined (Table 2), the stress-strain (σ-ε) relationship, and thereafter the tangent modulus ($Et = d\sigma/d\varepsilon$) at arbitrary stress levels could be calculated for each cornea. Table 3 presents the mean Et for each specimen group at three stress levels; 2kPa, 4kPa and 6kPa, and show significant reductions in Et in the Tra group, and the Taf group relative to the control specimens ($p< 0.01$ at all three stress levels considered). On the other hand, Tra and Taf groups exhibited similar Et values with no significant differences detected at the three stress levels (all $p> 0.80$).

3.4 Histological Analysis

No significant differences in fibril diameter were found among the three specimen groups ($p= 0.769$) through the analysis of transmission electron microscopy images (Figure 3 and Table 4). On the other hand, interfibrillar spacing exhibited large and significant differences ($p= 0.00$), being higher in the Tra and Taf groups by 21.9% and 23.6% (indicating lower fibril

density) compared with the control group.

Discussion

Due to their effectiveness in lowering IOP [27], PGF2α have become widely used in glaucoma management despite their reported side effects including conjunctival hyperemia [28], ocular irritation [29], iris pigmentation [30], and eyelid skin darkening [31]. While several studies have dealt with these biological effects [16, 32], few studies considered the PGF2α's influence on corneal biomechanics. Using corneal inflation testing in this study, large, consistent and significant decreases in corneal stiffness (as measured by the tangent modulus, Et) were found in ex-vivo rabbit eyes treated with Travoprost and Tafluprost, compared with control specimens.

Travoprost and Tafluprost are two types of PGF2α available for clinical use to lower IOP. They employ different mechanisms involving diverse receptor subtypes [33, 34], which induce differential expression of MMPs in the ciliary body or ciliary muscles [35, 36]. However, despite these differences, Travoprost and Tafluprost have been reported to exhibit similar effects in IOP reduction [37], and have been shown in this study to induce similar changes in corneal biomechanics.

The changes in corneal biomechanics may be attributed to the effects of PGF2α on the extracellular matrix of corneal stroma via upregulation of MMP [38]. In addition, PGF2α therapy can increase the keratocyte density in the stroma, probably due to the diminished extracellular matrix owing to the activation of MMP and inhibition of their tissue inhibitors [39].

Previous studies on the biomechanical effects of PGF2α used the Ocular Response Analyzer (ORA) to provide indications of behavior change. All studies [40-43], except one [44], reported increases in the Corneal Hysteresis parameter (CH – parameter linked with cornea's dynamic damping) with PGF2α treatment. However, the image with the Corneal Resistance Factor (CRF – linked with mechanical stiffness) was less clear with reported decreases [43,

44] and no significant changes [40] [42]. Further, after adjusting for factors that potentially influence corneal dynamic parameters, a significant difference was detected in the deformation amplitude (DA) parameter – indicating stiffness reduction – in a device based on Corneal Visualization Scheimpflug Technology (Corvis ST) post PGF2α therapy [45].

However, as the biomechanical metrics provided by the ORA and Corvis ST can be influenced by factors such as IOP and corneal thickness [15, 46-49], and since the link between the CH, CRF and DA metrics and the established mechanical properties of tissue (such as tangent modulus) has not been established yet, it is difficult to extract clear conclusions on the effect of PGF2α on corneal biomechanical properties based on these studies. For this reason, inflation testing, which provides direct measurement of the tissue's properties has been adopted in this study.

Inflation testing is considered superior to the commonly-used strip extensometry testing [50, 51] as it subjects the cornea to posterior pressure simulating IOP, keeps the cornea intact, maintains tissue hydration, adopts boundary conditions that approximate connection to the stiffer limbus, and enables monitoring of specimen deformation using non-contact methods. The initial topography measurements enable the construction of specimen-specific numerical models, and inverse analysis can be used to derive the tissue's material properties in forms of stress-strain behavior and hence the tangent modulus at different stress or strain levels based on the experimentally-obtained pressure deformation results.

In our study, all specimens exhibited clear nonlinear mechanical behavior, and the results show large, consistent and significant stiffness decreases in the treated groups. The tangent modulus was consistently lower in the Tra and Taf groups compared to the control group (by 32.7% and 31.2% at 2 kPa stress, 30.0% and 30.1% at 4 kPa stress, 29.2% and 29.8% at 6 kPa stress). Meanwhile, corneal thickness decreased by 6.6% and 8.2% compared with the control group. The histological results also showed a significant increase in collagen interfibrillar spacing in the Tra and Taf groups (by 21.9% and 23.6%), indicating a decrease in collagen fibril density in the corneal stroma. However, there was no significant change in

fibril diameter after treatment. It is interesting to find that the change in CCT and fibril spacing tie with the stiffness change. While the change in corneal microstructure can lead to stiffness reduction (as collagen fibrils are the main load carrying components of the cornea), it has been theorized that PGF2α could stimulate collagen gel contraction [52], decrease fibronectin protein content [53], accelerate collagen degradation [54] and change stromal collagen distribution [53], all of which can cause tissue stiffness deterioration.

Changes in corneal biomechanics, such as those reported herein, can cause an underestimation in the measurement of IOP in tonometry. Because most tonometry methods rely on loading the cornea by contact or non-contact force and correlating the corneal deformation to the value of IOP, reducing corneal stiffness can lead to underestimations of IOP [55]. This is an interesting outcome since PGF2α are intended in the first place to lower IOP, but the long-term reductions in corneal stiffness may exaggerate the drop in IOP and overstate the effectiveness of the treatment.

There has been a significant thickness increase observed in all specimen groups during the storage period. This increase was most likely caused by the storage medium that can result in an anaerobic state and increased lacate concentrations [56], both of which may promote tissue swelling during the storage period. This thickness increase could have masked a decrease in thickness caused by storage in Travoprost and Tafluprost similar to what has been observed in clinical studies involving patients with glaucoma or ocular hypertension [12, 13].

The study has a number of limitations including the use of rabbit eyes as models of the human eye. This has been necessary due to the difficulties in obtaining sufficient human donor eyes, and justified by findings of similarity of biomechanical behavior with human eyes in earlier experimental studies [57, 58]. Corneal tissue was separated from the sclera and stored in Eusol-C for ten days due to difficulties in storing the eye globes intact. Corneal separation would expose to treatment the interior side of the corneoscleral tissue as well as the edge of the cut, and would create conditions that were different from the physiological state Furthermore, since differences are possible between ex-vivo and in-vivo tissue behavior,

it may be difficult to correlate directly the findings of the present study with what to expect in clinical practice. However, it was necessary to rely in this study on ex-vivo tissue due to the current inability to measure corneal mechanical behavior in vivo.

Using a standard biomechanical test, this study investigated the effect of PGF2α hypotensive medication on corneal biomechanical properties. In conclusion, the results of the study demonstrate significant corneal material stiffness reductions associated with the use of PGF2α analogues (Travoprost diluent, 0.0004%; and Tafluprost diluent, 0.00015%). These results warrant caution when clinicians assess accuracy and adequacy of IOP control in glaucoma patients under chronic PGF2α therapy.

References:

1. Quigley, H. A.; Broman, A. T., The number of people with glaucoma worldwide in 2010 and 2020. *Br J Ophthalmol* **2006,** 90, (3), 262-7.
2. Ogden, R. W., *Non-linear elastic deformations*. Dover Publications, Inc: Mineola, New York 1997.
3. INVESTIGATORS., T. A., The Advanced Glaucoma Intervention Study (AGIS): 7. The relationship between control of intraocular pressure and visual field deterioration.The AGIS Investigators. *Am J Ophthalmol* **2000,** 130, (4), 429-40.
4. Camras, C. B., Comparison of latanoprost and timolol in patients with ocular hypertension and glaucoma: a six-month masked, multicenter trial in the United States. The United States Latanoprost Study Group. *Ophthalmology* **1996,** 103, (1), 138-47.
5. Lindsey, J. D.; Kashiwagi, K.; Boyle, D.; Kashiwagi, F.; Firestein, G. S.; Weinreb, R. N., Prostaglandins increase proMMP-1 and proMMP-3 secretion by human ciliary smooth muscle cells. *Curr Eye Res* **1996,** 15, (8), 869-75.
6. Schachtschabel, U.; Lindsey, J. D.; Weinreb, R. N., The mechanism of action of prostaglandins on uveoscleral outflow. *Curr Opin Ophthalmol* **2000,** 11, (2), 112-5.
7. Weinreb, R. N.; Lindsey, J. D.; Marchenko, G.; Marchenko, N.; Angert, M.; Strongin, A., Prostaglandin FP agonists alter metalloproteinase gene expression in sclera. *Invest Ophthalmol Vis Sci* **2004,** 45, (12), 4368-77.
8. Sagara, T.; Gaton, D. D.; Lindsey, J. D.; Gabelt, B. T.; Kaufman, P. L.; Weinreb, R. N., Topical prostaglandin F2alpha treatment reduces collagen types I, III, and IV in the monkey uveoscleral outflow pathway. *Arch Ophthalmol* **1999,** 117, (6), 794-801.
9. Tamm, E.; Lutjen-Drecoll, E.; Rohen, J. W., Age-related changes of the ciliary muscle in comparison with changes induced by treatment with prostaglandin F2 alpha. An ultrastructural study in rhesus and cynomolgus monkeys. *Mechanisms of ageing and development* **1990,** 51, (2), 101-20.
10. Lee, P. Y.; Podos, S. M.; Severin, C., Effect of prostaglandin F2 alpha on aqueous humor dynamics of rabbit, cat, and monkey. *Invest Ophthalmol Vis Sci* **1984,** 25, (9), 1087-93.
11. Gabelt, B. T.; Kaufman, P. L., Prostaglandin F2 alpha increases uveoscleral outflow in the cynomolgus

monkey. *Exp Eye Res* **1989,** 49, (3), 389-402.

12. Schlote, T.; Tzamalis, A.; Kynigopoulos, M., Central corneal thickness during treatment with travoprost 0.004% in glaucoma patients. *J Ocul Pharmacol Ther* **2009,** 25, (5), 459-62.
13. Zhong, Y.; Shen, X.; Yu, J.; Tan, H.; Cheng, Y., The comparison of the effects of latanoprost, travoprost, and bimatoprost on central corneal thickness. *Cornea* **2011,** 30, (8), 861-4.
14. Panos, G. D.; Konstantinidis, A.; Mendrinos, E.; Kozobolis, V.; Perente, I.; Gatzioufas, Z., Effect of tafluprost 0.0015% on central corneal thickness in patients with primary open-angle glaucoma. *Curr Eye Res* **2013,** 38, (9), 977-82.
15. Bao, F.; Deng, M.; Wang, Q.; Huang, J.; Yang, J.; Whitford, C.; Geraghty, B.; Yu, A.; Elsheikh, A., Evaluation of the relationship of corneal biomechanical metrics with physical intraocular pressure and central corneal thickness in ex vivo rabbit eye globes. *Exp Eye Res* **2015,** 137, 11-7.
16. Guenoun, J. M.; Baudouin, C.; Rat, P.; Pauly, A.; Warnet, J. M.; Brignole-Baudouin, F., In vitro comparison of cytoprotective and antioxidative effects of latanoprost, travoprost, and bimatoprost on conjunctiva-derived epithelial cells. *Invest Ophthalmol Vis Sci* **2005,** 46, (12), 4594-9.
17. Guenoun, J. M.; Baudouin, C.; Rat, P.; Pauly, A.; Warnet, J. M.; Brignole-Baudouin, F., In vitro study of inflammatory potential and toxicity profile of latanoprost, travoprost, and bimatoprost in conjunctiva-derived epithelial cells. *Invest Ophthalmol Vis Sci* **2005,** 46, (7), 2444-50.
18. Ni, S.; Yu, J.; Bao, F.; Li, J.; Elsheikh, A.; Wang, Q., Effect of glucose on the stress-strain behavior of ex-vivo rabbit cornea. *Exp Eye Res* **2011,** 92, (5), 353-60.
19. Bao, F.; Deng, M.; Zheng, X.; Li, L.; Zhao, Y.; Cao, S.; Yu, A. Y.; Wang, Q.; Huang, J.; Elsheikh, A., Effects of diabetes mellitus on biomechanical properties of the rabbit cornea. *Exp Eye Res* **2017,** 161, 82-8.
20. Bao, F.; Zheng, Y.; Liu, C.; Zheng, X.; Zhao, Y.; Wang, Y.; Li, L.; Wang, Q.; Chen, S.; Elsheikh, A., Changes in Corneal Biomechanical Properties With Different Corneal Cross-linking Irradiances. *J Refract Surg* **2018,** 34, (1), 51-58.
21. Yu, J. G.; Bao, F. J.; Joda, A.; Fu, X. A.; Zhou, S.; Wang, J.; Hu, X. L.; Wang, Q. M.; Elsheikh, A., Influence of glucocorticosteroids on the biomechanical properties of in-vivo rabbit cornea. *J Mech Behav Biomed Mater* **2014,** 29, 350-9.
22. Zheng, X.; Bao, F.; Geraghty, B.; Huang, J.; Yu, A.; Wang, Q., High intercorneal symmetry in corneal biomechanical metrics. *Eye and vision* **2016,** 3, 7.
23. Mulhern, M. G.; Condon, P. I.; O'Keefe, M., Myopic and hyperopic laser in situ keratomileusis retreatments: indications, techniques, limitations, and results. *J Cataract Refract Surg* **2001,** 27, (8), 1278-87.
24. Grupcheva, C. N.; Malik, T. Y.; Craig, J. P.; McGhee, C. N., In vivo confocal microscopy of corneal epithelial ingrowth through a laser in situ keratomileusis flap buttonhole. *J Cataract Refract Surg* **2001,** 27, (8), 1318-22.
25. Dhaliwal, D. K.; Romanowski, E. G.; Yates, K. A.; Hu, D.; Mah, F. S.; Fish, D. N.; Gordon, Y. J., Valacyclovir inhibition of recovery of ocular herpes simplex virus type 1 after experimental reactivation by laser in situ keratomileusis. *J Cataract Refract Surg* **2001,** 27, (8), 1288-93.
26. Wollensak, G.; Wilsch, M.; Spoerl, E.; Seiler, T., Collagen fiber diameter in the rabbit cornea after collagen crosslinking by riboflavin/UVA. *Cornea* **2004,** 23, (5), 503-7.
27. Al-Jazzaf, A. M.; DeSantis, L.; Netland, P. A., Travoprost: a potent ocular hypotensive agent. *Drugs Today (Barc)* **2003,** 39, (1), 61-74.
28. Stewart, W. C.; Kolker, A. E.; Stewart, J. A.; Leech, J.; Jackson, A. L., Conjunctival hyperemia in healthy subjects after short-term dosing with latanoprost, bimatoprost, and travoprost. *Am J Ophthalmol* **2003,**

135, (3), 314-20.

29. Day, D. G.; Sharpe, E. D.; Atkinson, M. J.; Stewart, J. A.; Stewart, W. C., The clinical validity of the treatment satisfaction survey for intraocular pressure in ocular hypertensive and glaucoma patients. *Eye (Lond)* **2006,** 20, (5), 583-90.
30. Huang, P.; Zhong, Z.; Wu, L.; Liu, W., Increased iridial pigmentation in Chinese eyes after use of travoprost 0.004%. *J Glaucoma* **2009,** 18, (2), 153-6.
31. Yang, H. K.; Park, K. H.; Kim, T. W.; Kim, D. M., Deepening of eyelid superior sulcus during topical travoprost treatment. *Jpn J Ophthalmol* **2009,** 53, (2), 176-9.
32. Kahook, M. Y.; Ammar, D. A., In vitro toxicity of topical ocular prostaglandin analogs and preservatives on corneal epithelial cells. *J Ocul Pharmacol Ther* **2010,** 26, (3), 259-63.
33. Woodward, D. F.; Regan, J. W.; Lake, S.; Ocklind, A., The molecular biology and ocular distribution of prostanoid receptors. *Surv Ophthalmol* **1997,** 41 Suppl 2, S15-21.
34. Ishida, N.; Odani-Kawabata, N.; Shimazaki, A.; Hara, H., Prostanoids in the therapy of glaucoma. *Cardiovasc Drug Rev* **2006,** 24, (1), 1-10.
35. Ooi, Y. H.; Oh, D. J.; Rhee, D. J., Effect of bimatoprost, latanoprost, and unoprostone on matrix metalloproteinases and their inhibitors in human ciliary body smooth muscle cells. *Invest Ophthalmol Vis Sci* **2009,** 50, (11), 5259-65.
36. Yamada, H.; Yoneda, M.; Gosho, M.; Kato, T.; Zako, M., Bimatoprost, latanoprost, and tafluprost induce differential expression of matrix metalloproteinases and tissue inhibitor of metalloproteinases. *BMC Ophthalmol* **2016,** 16, 26.
37. Takagi, Y.; Santo, K.; Hashimoto, M.; Fukuchi, T., Ocular hypotensive effects of prostaglandin analogs in Japanese patients with normal-tension glaucoma: a literature review. *Clin Ophthalmol* **2018,** 12, 1837-1844.
38. Viestenz, A.; Martus, P.; Schlotzer-Schrehardt, U.; Langenbucher, A.; Mardin, C. Y., [Impact of prostaglandin-F(2alpha)-analogues and carbonic anhydrase inhibitors on central corneal thickness -- a cross-sectional study on 403 eyes]. *Klin Monbl Augenheilkd* **2004,** 221, (9), 753-6.
39. Bergonzi, C.; Giani, A.; Blini, M.; Marchi, S.; Luccarelli, S.; Staurenghi, G., Evaluation of prostaglandin analogue effects on corneal keratocyte density using scanning laser confocal microscopy. *J Glaucoma* **2010,** 19, (9), 617-21.
40. Tsikripis, P.; Papaconstantinou, D.; Koutsandrea, C.; Apostolopoulos, M.; Georgalas, I., The effect of prostaglandin analogs on the biomechanical properties and central thickness of the cornea of patients with open-angle glaucoma: a 3-year study on 108 eyes. *Drug design, development and therapy* **2013,** 7, 1149-56.
41. Agarwal, D. R.; Ehrlich, J. R.; Shimmyo, M.; Radcliffe, N. M., The relationship between corneal hysteresis and the magnitude of intraocular pressure reduction with topical prostaglandin therapy. *Br J Ophthalmol* **2012,** 96, (2), 254-7.
42. Lazcano-Gomez, G.; Ancona-Lezama, D.; Gil-Carrasco, F.; Jimenez-Roman, J., Effects of topical travoprost 0.004% on intraocular pressure and corneal biomechanical properties in an animal model. *Digital journal of ophthalmology : DJO / sponsored by Massachusetts Eye and Ear Infirmary* **2016,** 22, (1), 1-5.
43. Detry-Morel, M.; Jamart, J.; Pourjavan, S., Evaluation of corneal biomechanical properties with the Reichert Ocular Response Analyzer. *Eur J Ophthalmol* **2011,** 21, (2), 138-48.
44. Meda, R.; Wang, Q.; Paoloni, D.; Harasymowycz, P.; Brunette, I., The impact of chronic use of prostaglandin analogues on the biomechanical properties of the cornea in patients with primary

open-angle glaucoma. *Br J Ophthalmol* **2017,** 101, (2), 120-125.

45. Wu, N.; Chen, Y.; Yu, X.; Li, M.; Wen, W.; Sun, X., Changes in Corneal Biomechanical Properties after Long-Term Topical Prostaglandin Therapy. *PLoS One* **2016,** 11, (5), e0155527.
46. Kotecha, A.; Elsheikh, A.; Roberts, C. R.; Zhu, H.; Garway-Heath, D. F., Corneal thickness- and age-related biomechanical properties of the cornea measured with the ocular response analyzer. *Invest Ophthalmol Vis Sci* **2006,** 47, (12), 5337-47.
47. Chang, P. Y.; Chang, S. W.; Wang, J. Y., Assessment of corneal biomechanical properties and intraocular pressure with the Ocular Response Analyzer in childhood myopia. *Br J Ophthalmol* **2010,** 94, (7), 877-81.
48. Sullivan-Mee, M.; Billingsley, S. C.; Patel, A. D.; Halverson, K. D.; Alldredge, B. R.; Qualls, C., Ocular Response Analyzer in subjects with and without glaucoma. *Optometry Vision Sci* **2008,** 85, (6), 463-470.
49. Tas, M.; Oner, V.; Ozkaya, E.; Durmus, M., Evaluation of corneal biomechanical properties in patients with rheumatoid arthritis: a study by ocular response analyzer. *Ocul Immunol Inflamm* **2014,** 22, (3), 224-7.
50. Hoeltzel, D. A.; Altman, P.; Buzard, K.; Choe, K., Strip extensiometry for comparison of the mechanical response of bovine, rabbit, and human corneas. *J Biomech Eng* **1992,** 114, (2), 202-15.
51. Elsheikh, A.; Anderson, K., Comparative study of corneal strip extensometry and inflation tests. *J R Soc Interface* **2005,** 2, (3), 177-85.
52. Liu, Y.; Yanai, R.; Lu, Y.; Hirano, S.; Sagara, T.; Nishida, T., Effects of antiglaucoma drugs on collagen gel contraction mediated by human corneal fibroblasts. *J Glaucoma* **2006,** 15, (3), 255-9.
53. Wu, K. Y.; Wang, H. Z.; Hong, S. J., Effect of latanoprost on cultured porcine corneal stromal cells. *Curr Eye Res* **2005,** 30, (10), 871-9.
54. Maruyama, Y.; Mori, K.; Ikeda, Y.; Ueno, M.; Kinoshita, S., Effects of long-term topical prostaglandin therapy on central corneal thickness. *J Ocul Pharmacol Ther* **2014,** 30, (5), 440-4.
55. Liu, J.; Roberts, C. J., Influence of corneal biomechanical properties on intraocular pressure measurement: quantitative analysis. *J Cataract Refract Surg* **2005,** 31, (1), 146-55.
56. Redbrake, C.; Salla, S.; Frantz, A.; Reim, M., [Energy metabolism of the human cornea in various culture systems]. *Klin Monbl Augenheilkd* **1997,** 210, (4), 213-8.
57. Sjoquist, B.; Basu, S.; Byding, P.; Bergh, K.; Stjernschantz, J., The pharmacokinetics of a new antiglaucoma drug, latanoprost, in the rabbit. *Drug Metab Dispos* **1998,** 26, (8), 745-54.
58. Pellinen, P.; Huhtala, A.; Tolonen, A.; Lokkila, J.; Maenpaa, J.; Uusitalo, H., The cytotoxic effects of preserved and preservative-free prostaglandin analogs on human corneal and conjunctival epithelium in vitro and the distribution of benzalkonium chloride homologs in ocular surface tissues in vivo. *Curr Eye Res* **2012,** 37, (2), 145-54.

Figure Captions

Figure 1 Corneal profile (A) captured before the start of the inflation test by one of the three cameras mounted on the inflation rig (B) and used to construct specimen-specific numerical models (C)

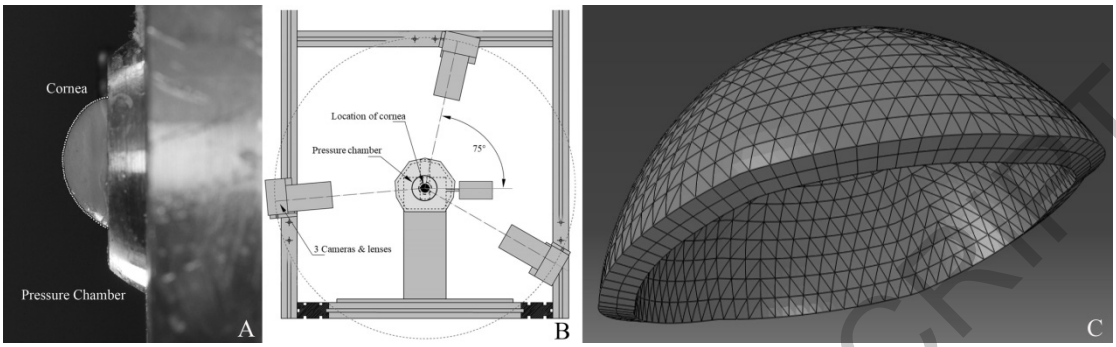

Figure 2 Pressure-displacement behavior at the corneal apex of one typical specimen during the 4 loading cycles

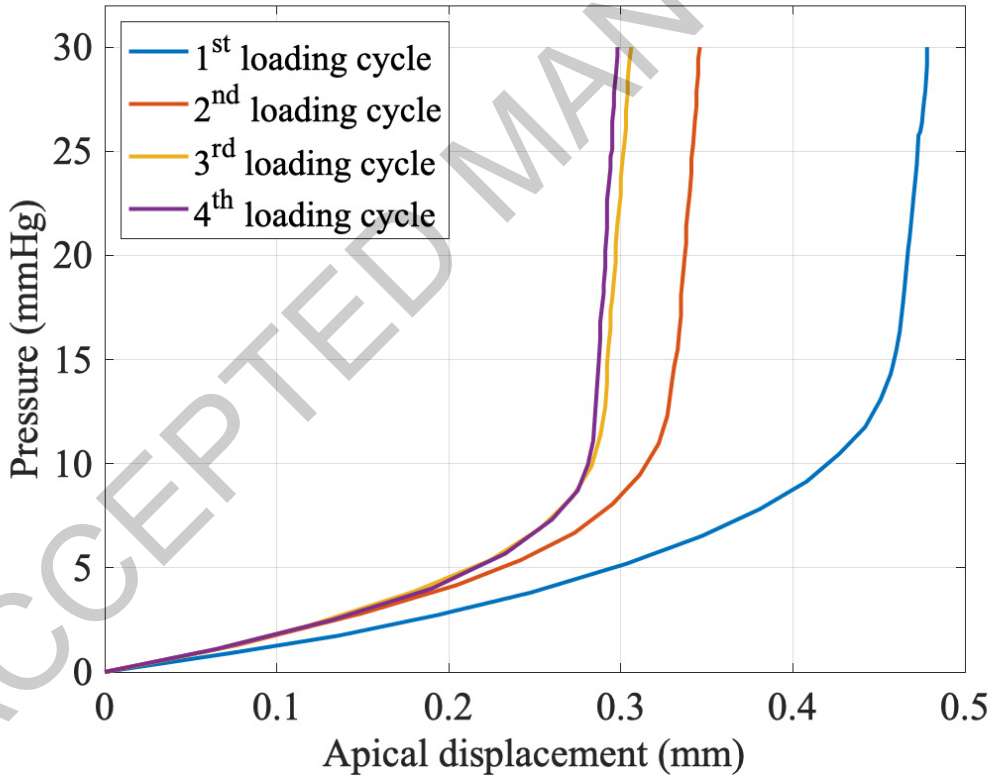

Figure 3 Mean pressure-displacement behavior at the corneal apex in the three groups

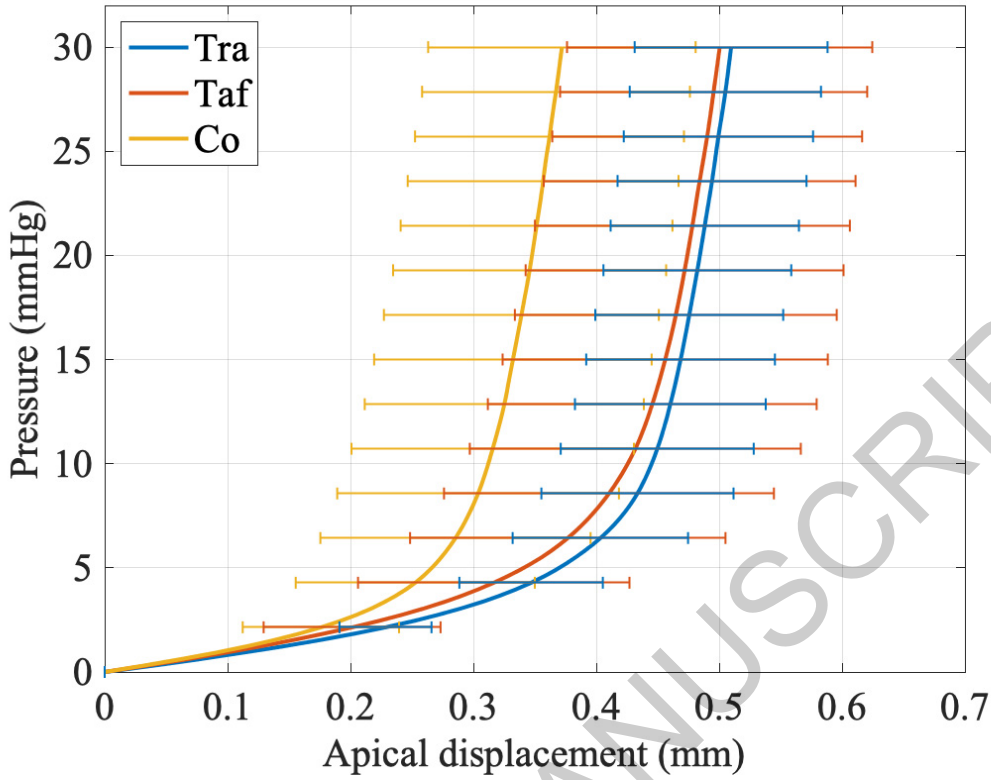

Figure 4 Cross-sectional images of corneal stroma showing collagen fibrils obtained using TEM with 40,000 magnification. (A) Travoprost Treated Group, (B) Tafluprost Treated Group, (C) Control group

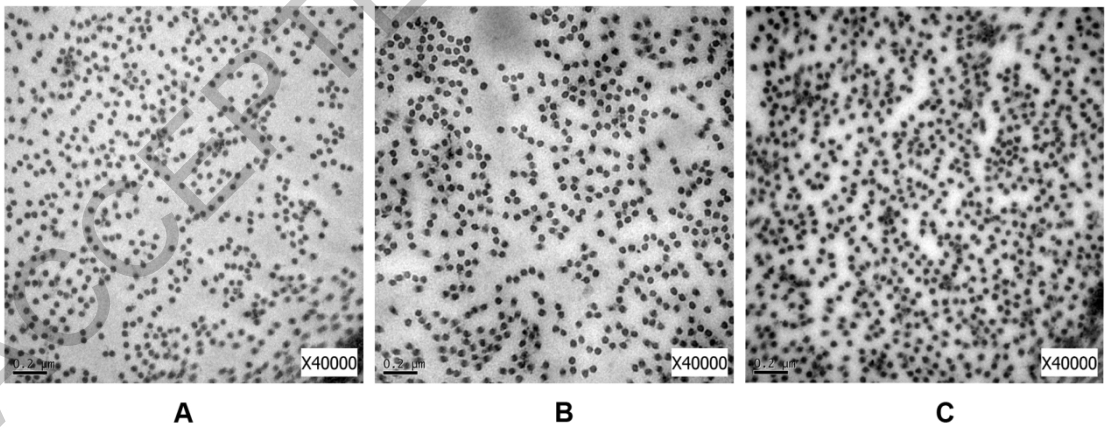

Table Captions

Table 1 Constitutive parameters α and μ obtained for 3 specimens using different initial values in the inverse analysis

Table 2 Mean and standard deviation of constitutive parameters α and μ in the three specimen groups

Table 3 Average and standard deviation values of tangent modulus in the three groups at different stress levels

Table 4 Mean and standard deviation of interfibrillar spacing and fibril diameter in corneal stroma in the three specimen groups

Table 1 Constitutive parameters α and μ obtained for 3 specimens using different initial values in the inverse analysis

Inverse attempts	Initial values		Tra case			Taf case			Co case		
			Obtained values		RMS (μm)	Obtained values		RMS (μm)	Obtained values		RMS (μm)
	μ	α	μ	α		μ	α		μ	α	
1	0.001	90	0.0426	105.29	12.02	0.0140	38.97	18.20	0.0044	49.75	29.49
2	0.002	180	0.0427	105.21	11.96	0.0140	38.97	18.20	0.0044	49.75	29.49
3	0.0005	45	0.0426	105.29	12.02	0.0140	38.98	18.19	0.0044	49.75	29.49
4	0.002	45	0.0427	105.21	11.96	0.0140	38.97	18.20	0.0044	49.75	29.49
5	0.0005	180	0.0427	105.21	11.96	0.0140	38.98	18.20	0.0044	49.75	29.49

Tra = Travoprost treated group, Taf = Tafluprost treated group, Co = control group

Table 2 Mean and standard deviation of constitutive parameters α and μ in the three specimen groups

Group	α	μ	RMS, μm
Tra	59.44±19.44	0.0044±0.0043	47.15±27.79
Taf	58.03±19.72	0.0070±0.0107	42.42±29.56
Co	80.24±21.16	0.0123±0.0145	37.56±20.74

Tra = Travoprost treated group, Taf = Tafluprost treated group, Co = control group

Table 3 Mean and standard deviation of tangent modulus (Et) in the three groups at different stress levels

Stress (kPa)	Tangent Modulus, Et (MPa)			p	Et_{Tra}/Et_{Co} %	Et_{Taf}/Et_{Co} %
	Tra	Taf	Co			
2.0	0.12±0.03	0.12±0.05	0.17±0.05	0.00	67.3	68.8
4.0	0.22±0.07	0.22±0.08	0.32±0.08	0.00	70.0	69.9
6.0	0.33±0.11	0.33±0.12	0.46±0.12	0.00	70.8	70.2

Tra = Travoprost treated group, Taf = Tafluprost treated group, Co = control group; Et_{Tra}/Et_{Co} = ratio between tangent modulus in Travoprost treated group (Et_{Tra}) and control group (Et_{Co}); Et_{Taf}/Et_{Co} = ratio between tangent modulus in Tafluprost treated group (Et_{Taf}) and control group (Et_{Co})

Table 4 Mean and standard deviation of interfibrillar spacing and fibril diameter in corneal stroma in the three specimen groups

Group	n	Fibril diameter (nm)	Interfibrillar spacing (nm)
Tra	8	30.92±1.35	44.28±1.67
Taf	8	31.18±0.56	44.90±3.65
Co	8	30.78±1.24	36.33±4.62
Tra/C_o %	-	100.4	121.9
Taf/C_o %	-	101.3	123.6

Tra = Travoprost treated group, Taf = Tafluprost treated group, Co = Control group.